
Numerical Studies of Counterflow Turbulence Velocity Distribution of Vortices

Hiroyuki Adachi · Makoto Tsubota

Received: date / Accepted: date

Abstract We performed the numerical simulation of quantum turbulence produced by thermal counterflow in superfluid ^4He by using the vortex filament model. The pioneering work was made by Schwarz, which has two defects. One is neglecting non-local terms of the Biot-Savart integral (localized induction approximation, LIA), and the other is the unphysical mixing procedure in order to sustain the statistically steady state of turbulence. We succeeded in making the statistically steady state without the LIA and the mixing. This state shows the characteristic relation $L = \gamma^2 v_{ns}^2$ between the line-length-density L and the counterflow relative velocity v_{ns} with the quantitative agreement of the coefficient γ with some typical observations. We compare our numerical results to the observation of experiment by Paoletti *et al*, where thermal counterflow was visualized by solid hydrogen particles.

Keywords superfluid ^4He · quantized vortices · counterflow

1 Introduction

Quantum turbulence (QT), which consists of a tangle of quantized vortices, has been investigated since the thermal counterflow experiments of Vinen [1-4] half a century ago, while the underlying physics is far from being fully understood [5,6]. The numerical simulations are the useful source of knowledge about QT, because the whole dynamics of this system is too complicated to be described analytically. One of the powerful schemes of the simulation is the vortex filament model based on pioneering works by Schwarz [7,8]. Schwarz performed the numerical simulation of counterflow turbulence under the periodic boundary condition by using the localized induction approximation (LIA) which neglects a non-local term of the Biot-Savart integral [8]. However he could not obtain the statistically steady state (SSS) because the vortices lie in planes normal to $\mathbf{v}_{ns} = \mathbf{v}_n - \mathbf{v}_s$ to prevent them from reconnecting. Therefore the unphysical mixing

H.Adachi , M.Tsubota
Department of Physics, Osaka City University, Sumiyoshi-Ku, Osaka 558-885
Tel.: +81-6-6605-3073
Fax: +81-6-6605-2522
E-mail: adachi@sci.osaka-cu.ac.jp

procedure, in which half of the vortices are randomly selected to be rotated by 90° around the axis defined by the flow velocity, was used, and only this method enabled him to obtain the SSS. This failure reminds us that the LIA is unsuitable through the absence of the interaction between vortices. Recently, thermal counterflow in superfluid ^4He was visualized by using solid hydrogen particles, and the velocity distribution of particles was observed [9]. In this experiment, two types of particles appeared. Some particles move straight along the normalflow with the approximately same velocity as normalflow. Other particles move zigzag along the direction of superfluid and has different velocity from superfluid. In the latter case, particles seem to be trapped in the core of the vortices. We try to apply our numerical results for understanding these observations.

Section 2 describes the equation of motion of vortices and the method of numerical calculation. In Sec.3 we show the typical numerical results of vortex tangle. Section 4 studies the validity of the LIA by comparing the LIA calculation with the full Biot-Savart calculation. In the section 5 we present the velocity distribution of vortices in the SSS of vortex tangle and compare it with that of particles in the experimental observation.

2 Equations of Motion and Numerical Simulation

At 0K the velocity $\dot{\mathbf{s}}_0$ of the filament at the point $\mathbf{s}(\xi,t)$ is given by

$$\dot{\mathbf{s}}_0 = \frac{\kappa}{4\pi} \mathbf{s}' \times \mathbf{s}'' \ln\left(\frac{2(l_+l_-)^{1/2}}{e^{1/4}a_0}\right) + \frac{\kappa}{4\pi} \int_L' \frac{(\mathbf{s}_1 - \mathbf{s}) \times d\mathbf{s}_1}{|\mathbf{s}_1 - \mathbf{s}|^3} + \mathbf{v}_{s,a}, \quad (1)$$

where the prime denotes the derivatives with respect to the arc length ξ , and κ is the quantized circulation, a_0 is a cutoff parameter corresponding to a vortex core radius, l_+ and l_- are the length of the two adjacent line elements that hold the points between. The first term shows the localized induction field arising from a curved line element acting on itself. The second term represents the non-local field obtained by carrying out the integral of the Biot-Savart integral along the rest of the filament. The third term $\mathbf{v}_{s,a}$ is an applied field. The LIA used in some works (e.g.,[7,8,10,11]) means neglecting the second non-local term. In contrast the calculation without the LIA is called the full Biot-Savart calculation. At finite temperatures, the velocity $\dot{\mathbf{s}}$ is given by

$$\dot{\mathbf{s}} = \dot{\mathbf{s}}_0 + \alpha \mathbf{s}' \times (\mathbf{v}_n - \dot{\mathbf{s}}_0) - \alpha' \mathbf{s}' \times [\mathbf{s}' \times (\mathbf{v}_n - \dot{\mathbf{s}}_0)], \quad (2)$$

where α and α' are the temperature-dependent friction coefficients, \mathbf{v}_n is the normalfluid velocity, and $\dot{\mathbf{s}}_0$ is calculated from Eq.(1). In the work [8] the author neglected the third term of Eq.(2). We performed the full Biot-Savart calculation in this work. The concrete reconnection procedure used in this work is the following. Every vortex is represented by a string of points at intervals of almost $\delta\xi$. When a point on a vortex approaches another point on another vortex more closely than the fixed space resolution $\Delta\xi$, we join these two points and reconnect the vortices [12]. For the integration of the motion of Eq.(2) in time we used the classical 4th order Runnge-Kutta method. We usually start with an initial vortex configuration of six vortex rings as shown in Fig.1(upper left).

3 Simulation of Counterflow Turbulence

In this section we present the numerical simulations of counterflow turbulence at the temperature $T=1.9\text{K}$, in the computing box $0.1 \times 0.1 \times 0.1 \text{ cm}^3$, at applied counterflow velocity $v_{ns}=0.286, 0.381, 0.572 \text{ cm/s}$. A typical result is shown in Fig.1. Here the

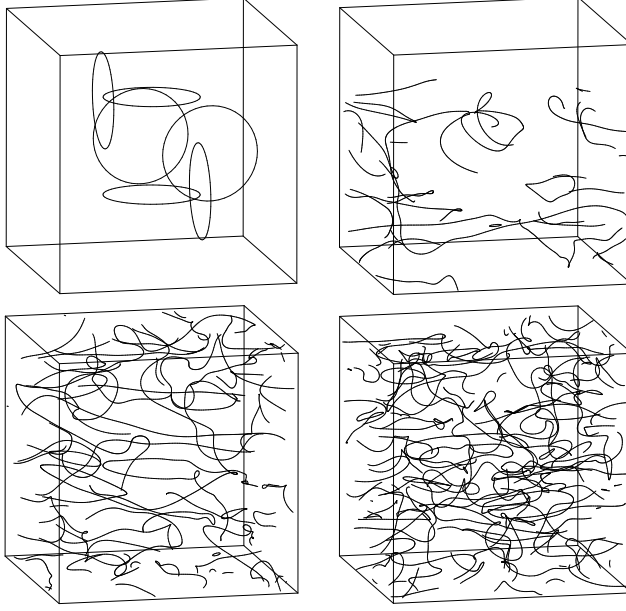


Fig. 1 Development of a vortex tangle by the full Biot-Savart calculation in a periodical box with the size 0.1 cm . Here temperature $T=1.9\text{K}$, and counterflow velocity $v_{ns}=0.572\text{cm/s}$ is along the vertical axis. Upper left $t=0 \text{ s}$, upper right $t=0.5 \text{ s}$, lower left $t=1.2 \text{ s}$, lower right $t=2.5 \text{ s}$

initial configuration of vortex loops evolves in the periodical box to a highly chaotic vortex tangle. The vortex line density $L(t)$ is defined as the vortex line length per unit volume. In Fig.2 we depict the time evolution of quantity $L(t)$. It is seen that the vortex tangle goes to the SSS after growth period. In Fig.2(b) we found out that line length density satisfied the characteristic relation $L = \gamma^2 v_{ns}^2$ which have been obtained in previous experiments [13]. This relation is derived from the Vinen's equation [3], and also obtained by Schwarz using the LIA and the dynamical scaling [8]. We obtain $\gamma \approx 139\text{s/cm}^2$ which quantitatively agrees with the experimental observation $\gamma \approx 130\text{s/cm}^2$ [14].

4 Validity of the LIA

In the similar works [8,10] the authors did not obtain the SSS of turbulence (the work [8] created the SSS only with the mixing.) The SSS was realized in the work [11] by

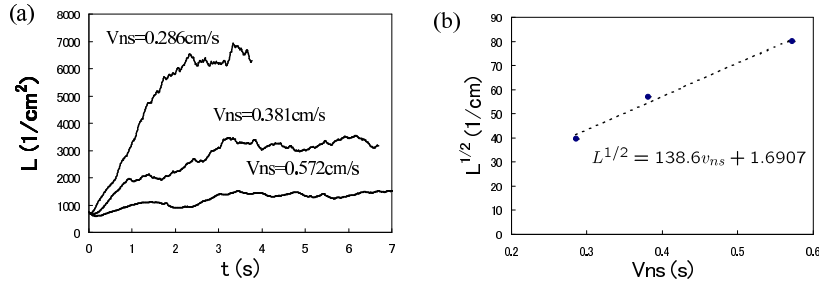


Fig. 2 Vortex line density as a function of time for different driving normalfluid \mathbf{v}_n equal to 0.286, 0.381, 0.572 cm/s

using the LIA, in which the authors mentioned that failures of previous works were due to the unsuitable reconnection procedure. We will discuss the main reason why the SSS was not realized in previous works. In order to consider the validity of the LIA, we compare two calculations. One uses the LIA [Fig.3 left], and the other uses the full Biot-Savart law [Fig.3 right]. We run both calculations at the temperature

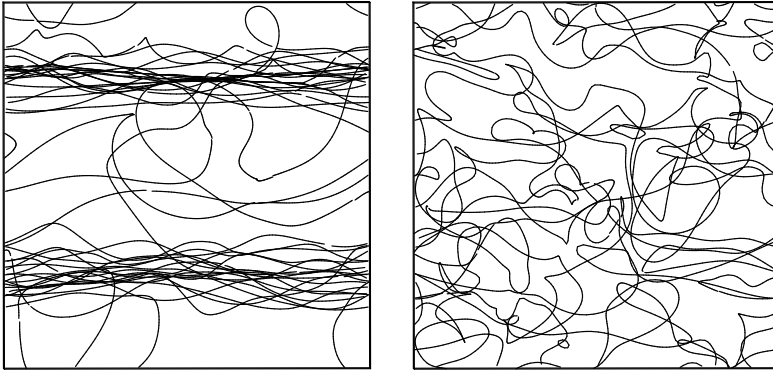


Fig. 3 Side view of vortex configuration by the LIA calculation (left) and by the full Biot-Savart law (right) at $t=34.5\text{s}$. The system is a $(0.2\text{cm})^3$ cube. Applied normalfluid velocity $v_{ns} = 0.367\text{cm/s}$.

$T=1.6\text{K}$, in the computing cubic box $0.2 \times 0.2 \times 0.2 \text{ cm}^3$, and applied counterflow velocity $v_{ns}=0.367\text{cm/s}$. To explain the difference between the results of the LIA and full Biot-Savart law we introduce the dimensionless anisotropy parameter [8]

$$I_{\parallel} = \frac{1}{\Omega L} \int_L [1 - (\mathbf{s}' \cdot \hat{\mathbf{r}}_{\parallel})^2] d\xi. \quad (3)$$

Here $\hat{\mathbf{r}}_{\parallel}$ stands for a unit vector parallel to the \mathbf{v}_{ns} direction, and Ω is the sample volume. An isotropic tangle yields $I_{\parallel} = 2/3$. At the other extreme, if the tangle consists

entirely of curves lying in planes normal to \mathbf{v}_{ns} , $\bar{I}_{||} = 1$. The time evolution of $L(t)$ and $I_{||}(t)$ is shown in Fig 4. Figure 3 (left) and Fig.4 (b) show that the many vortices lie

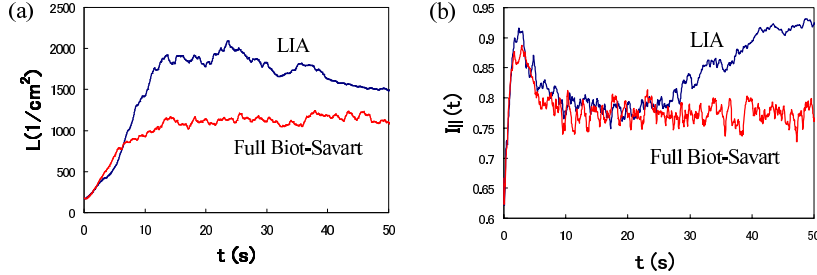


Fig. 4 Comparison of a vortex line density $L(t)$ (a) and an anisotropy parameter $I_{||}(t)$ (b).

in the planes normal to \mathbf{v}_{ns} , the vortex tangle being degenerate. Since the dense part of vortices catch other vortices moving freely, vortices become to huddle in periodical planes as shown in Fig.3 (left). This ill behavior comes from the mutual friction, which tends to expand vortices perpendicular to the \mathbf{v}_{ns} , so that vortices gradually lie in planes normal to \mathbf{v}_{ns} . However, a non-local term of the Biot-Savart integral could yield the velocity in a direction parallel to \mathbf{v}_{ns} even when vortices align in a plane perpendicular to \mathbf{v}_{ns} , thus destroying the ill structure. Hence, the calculation with the full Biot-Savart law can sustain the SSS in contrast to that with the LIA.

5 Velocity Distribution of Vortices

For comparison with experimental results [9], we present the velocity distributions of vortices in the SSS. We obtained the distributions as shown in [Fig.5 left] by measuring the z -component of the velocity $\dot{\mathbf{s}}$ at each points on the vortex filaments from the results of counterflow turbulence in which applied velocity \mathbf{v}_{ns} is directed to z -axis. The velocity $\dot{\mathbf{s}}$ does not necessarily express the particle motion on the vortex filament which probably occur in the experiments. Therefore we brought this effect in our calculation. For the sake of simplicity, suppose the trapped particles do not have a significant influence on the local motion of the lines, and that viscous interaction of a particle with the normal fluid causes the particles to move along the filament at a rate given by the Stokes law with the force equal to the component of the viscous force along the line. With these assumption, the z -component of the velocity $\dot{\mathbf{s}}_p$ including the effect of motion is derived from the similar fashion of the work [15] like

$$\dot{\mathbf{s}}_{pz} = \dot{\mathbf{s}}_n \cdot \hat{\mathbf{z}} + (v_n - \dot{\mathbf{s}}_n \cdot \hat{\mathbf{z}}) \cos^2 \theta, \quad (4)$$

where $\dot{\mathbf{s}}_n$ is the normal component of the vortex velocity to the vortex filament, θ is a polar angle of the vortex relative to \mathbf{v}_{ns} . The velocity distributions of both $\dot{\mathbf{s}}_z$ and $\dot{\mathbf{s}}_{pz}$ are shown in [Fig.5 right]. The vortices in our simulations have lower vertical velocities than the superfluid velocity just like the experimental observation. For the quantitative

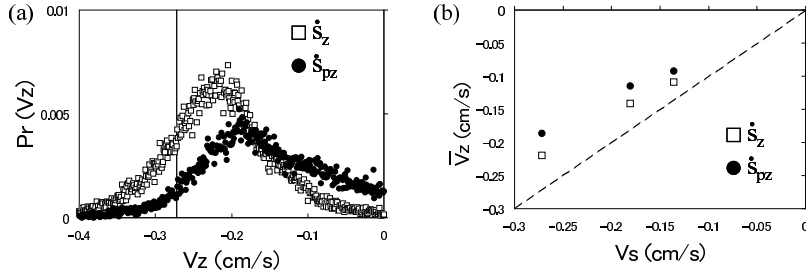


Fig. 5 (a) The vertical velocity v_z distribution at temperature $T=1.9$ K, applied velocity $v_{n,s}=0.572$ cm/s. The superfluid velocity v_s is shown by vertical line. (b) Vertical velocity of vortex tangle \bar{v}_z , which is a peak velocity of the distribution, as a function of v_s . The dashed line corresponds to $\bar{v}_z = v_s$.

agreement with observation, we need to introduce other effects such as a distortion of vortices by particles.

6 Conclusions

The obtained numerical results with the full Biot-Savart law demonstrate that the initially smooth vortex rings develop to a vortex tangle of the statistically steady state. We compared the numerical results by the full Biot-Savart calculation to that by the LIA calculation. The LIA calculation could not sustain the statistically steady state in contrast to the full Biot-Savart calculation. We compared the velocity distributions of vortices obtained by our numerical simulations to the observations by the visualization experiment of counterflow by using solid hydrogen particles. Our results agree with the experimental observation qualitatively in that most vortices have lower velocities than the superfluid velocity.

Acknowledgements We would like to thank M. S. Paoletti and D. P. Lathrop for giving their preliminary experimental data and the fruitful discussions.

References

1. W.F.Vinen, Proc. Roy. Soc. London A **240**, 114 (1957).
2. W.F.Vinen, Proc. Roy. Soc. London A **240**, 128 (1957).
3. W.F.Vinen, Proc. Roy. Soc. London A **242**, 493 (1957).
4. W.F.Vinen, Proc. Roy. Soc. London A **243**, 400 (1957).
5. M.Tsubota, J. Phys. Soc. Jpn. **77**, 111006 (2008).
6. Progres in Low Temperature Physics volume XVI, edited by W.P.Halperin and M.Tsubota, ELSEVIER, Amsterdam (2009).
7. K.W.Schwarz, Phys. Rev. B **31**, 5782 (1985).
8. K.W.Schwarz, Phys. Rev. B **38**, 2398 (1988).
9. M.S.Paoletti, R.B.Fiorito, K.R.Sreenivasan and D.P.Lathrop, J. Phys. Soc. Jpn. **77**, 111007 (2008).
10. R.G.M.Aarts, A numerical study of quantized vortices in HeII, Technishe Universiteit Eindhoven, Eindhoven (1993).

-
11. L.P.Kondaurova, V.A.Andryuschenko and S.K.Nemirovskii, *J. Low Temp. Phys.* **150**, 415 (2008).
 12. M.Tsubota, T.Araki and S.K.Nemirovskii, *Phys. Rev. B* **62**, 11751 (2000).
 13. J.T.Tough, *Progres in Low Temperature Physics volume VIII*, edited by D.F.Brewer, ELSEVIER, Amsterdam (2009).
 14. R.K.Childers and J.T.Tough, *Phys. Rev. B* **13**, 1040 (1976).
 15. D.R.Poole, C.F.Barengi, Y.A.Sergeev and W.F.Vinen, *Phys. Rev. B* **71**, 064514 (2005).